Shock wave study of the reaction HO2+HO2→H2O2+O2 : Confirmation of a rate constant minimum near 700 K

H. Hippler, J. Troe, and J. Willner

Citation: The Journal of Chemical Physics **93**, 1755 (1990); doi: 10.1063/1.459102
View online: http://dx.doi.org/10.1063/1.459102
View Table of Contents: http://scitation.aip.org/content/aip/journal/jcp/93/3?ver=pdfcov
Published by the AIP Publishing

Articles you may be interested in

Shock wave studies of the reactions HO+H2O2→H2O+HO2 and HO+HO2→H2O+O2 between 930 and 1680 K
J. Chem. Phys. **103**, 3510 (1995); 10.1063/1.470235

Theoretical characterization of the minimum energy path for the reaction H+O2→HO2*→HO+O
J. Chem. Phys. **88**, 6273 (1988); 10.1063/1.454466

Reaction rate constants of HO2+O3 in the temperature range 233–400 K
J. Chem. Phys. **88**, 896 (1988); 10.1063/1.454169

Studies of reactions of importance in the stratosphere. III. Rate constant and products of the reaction between ClO and HO2 radicals at 298 K
J. Chem. Phys. **72**, 2364 (1980); 10.1063/1.439484

Rate constant of the reaction HO2+ClO→HOCl+O2
J. Chem. Phys. **69**, 2925 (1978); 10.1063/1.436850

This article is copyrighted as indicated in the article. Reuse of AIP content is subject to the terms at: http://scitation.aip.org/termsconditions. Downloaded to IP: 130.102.42.98 On: Sun, 23 Nov 2014 05:25:21

Shock wave study of the reaction $HO_2 + HO_2 \rightarrow H_2O_2 + O_2$: Confirmation of a rate constant minimum near 700 K

H. Hippler, J. Troe, and J. Willner
Institut für Physikalische Chemie, Universität Göttingen, Tammannstrasse 6, D-3400 Göttingen, West Germany

(Received 15 February 1990; accepted 2 April 1990)

The HO_2 self-reaction $HO_2 + HO_2 \rightarrow H_2O_2 + O_2$ was studied in shock waves between 750 and 1120 K. Two different HO_2 sources were used, the thermal dissociation of $CH_3O_2CH_3$ in the presence of excess O_2 and the thermal dissociation of H_2O_2. The reaction is characterized by a curved Arrhenius plot of the rate constant k. The combination with low temperature data shows a deep minimum of k near 700 K. The rate constant, at 1 bar gas pressure, between 300 and 1100 K can be represented as $k/\text{cm}^3\,\text{mol}^{-1}\,\text{s}^{-1} = 4.2\times10^{14}\exp(-6030\,\text{K}/T) + 1.3\times10^{11}\exp(+820\,\text{K}/T)$. The first term in the present work was derived from measured ratios of k/ϵ and was evaluated with ϵ (HO_2, 230 nm, 1000 K) = 670 1 $\text{mol}^{-1}\,\text{cm}^{-1}$. Furthermore, a value of the rate constant of 3×10^{12} $\text{cm}^3\,\text{mol}^{-1}\,\text{s}^{-1}$ was derived near 1100 K for the reaction $HO + H_2O_2 \rightarrow HO_2 + H_2O$; for the reaction $HO + HO_2 \rightarrow H_2O + O_2$ a value of 3×10^{13} $\text{cm}^3\,\text{mol}^{-1}\,\text{s}^{-1}$ was obtained.

I. INTRODUCTION

The mutual reaction of two HO_2 radicals

$$HO_2 + HO_2 \rightarrow H_2O_2 + O_2 \quad (1)$$

presents a number of interesting aspects. Under atmospheric conditions[1,2] it constitutes the dominant source of H_2O_2 molecules, which afterwards photolyze via

$$H_2O_2 + h\nu \rightarrow 2HO, \quad (2)$$

or are attacked by HO via

$$HO + H_2O_2 \rightarrow H_2O + HO_2, \quad (3)$$

or disappear via rainout. The reaction also plays an important role in hydrogen and hydrocarbon oxidation,[3-5] particularly in high pressure combustion in the autoignition and knocking range at temperatures around 1000 K. Under these conditions, thermal decomposition of H_2O_2, i.e.,

$$H_2O_2 + M \rightarrow 2HO + M, \quad (4)$$

forms a dominant source of HO radicals which then attack the fuel molecules. Reaction (1), together with H atom abstraction from the fuel molecules by HO_2, here constitutes an important source of H_2O_2, and subsequently of HO radicals. It, therefore, directly contributes to the $H \rightarrow HO_2 \rightarrow OH$ sequence of the oxidation mechanism.

Reaction (1) has extensively been studied experimentally for the low temperature conditions of atmospheric interest (see summaries of earlier work in Refs. 1 and 2). The reaction shows a pressure dependence of the apparent rate constant with a nonvanishing component at "zero pressure." It also shows a marked negative temperature coefficient of the rate constant. These features have suggested[6,7] the intermediate formation of a cyclic hydrogen bonded intermediate HO_2HO_2. A mechanism of the type

$$HO_2 + HO_2 \rightarrow H_2O_4^* \rightarrow H_2O_2 + O_2, \quad (5)$$

$$H_2O_4^* + M \Leftrightarrow H_2O_4 + M, \quad (6)$$

was modeled. The possibilities of either two independent pathways, i.e., direct disproportionation and complex formation, or of one pathway only involving complex formation, have been discussed by RRKM theory on the basis of assumed structural features of H_2O_4. A very loose H_2O_4 had to be chosen in order to reconcile the low temperature observations.

The large number of careful experiments under low temperature conditions is in striking contrast to the scarcity of studies under combustion conditions. For about 20 years there was only one determination[8] of k_1 at temperatures above 1000 K, derived via HO_2 formation in reaction (3) after thermal decomposition (4) of H_2O_2 in shock waves. The high value of k_1 near 1200 K, in combination with room temperature measurements and information on the negative temperature coefficient of the rate constant, suggested a change of the temperature dependence with a deep minimum of k_1 somewhere between 300 and 1200 K. However, this conclusion was based on a single high temperature determination such that an independent confirmation appeared desirable. Recent measurements at intermediate temperatures[9] indeed showed indications of a rate constant minimum near 600 K. Nevertheless, a high temperature turnup of k_1 still had to be confirmed. This appeared particularly urgent in view of the recent emphasis of the largely neglected HO_2 reactions in high pressure combustion at temperatures between about 600 and 1200 K.[3-5] We, therefore, have undertaken a new study of reaction (1) in this temperature range, starting from the maximum temperatures attained in Ref. 9 and reaching up to the conditions of the old shock wave study of Ref. 8. Using an HO_2 source different from that of Ref. 8, the results both of Refs. 8 and 9 were confirmed and a strong positive temperature coefficient of k_1 between 800 and 1100 K was observed. We also repeated our studies of HO_2 formation in the thermal decomposition of H_2O_2, now using more modern techniques and more detailed evaluation methods, with the goal to compare results from two different HO_2 sources. The two approaches gave nicely consistent results confirming the high temperature turnup of k_1.

 0021-9606/90/151755-06$03.00 © 1990 American Institute of Physics

This article is copyrighted as indicated in the article. Reuse of AIP content is subject to the terms at: http://scitation.aip.org/termsconditions. Downloaded to IP: 130.102.42.98 On: Sun, 23 Nov 2014 05:25:21

With the available results, reaction (1) presents an impressive example of a complex-forming bimolecular reaction with a pronounced rate constant minimum. Similar cases without a pressure dependence are known, e.g., for some ion–molecule reaction such as[10] $CH_4 + O_2^+$; pressure dependent rate constants appear to be the rule for the HO attack of alkenes.[11,12] In the latter cases, the fate of the low temperature–high pressure adducts remains a largely unsolved problem.[1] This is also the case with reaction (1). The origin of rate constant minima in complex-forming bimolecular reactions, occuring with and without pressure dependences is discussed elsewhere.[13]

II. EXPERIMENTAL TECHNIQUE

Our experiments were performed in reflected shock waves using UV absorption spectroscopy in order to follow HO_2 and H_2O_2 concentration profiles. HO profiles were measured behind incident waves. Our aluminum shock tube had an internal diameter of 10 cm and a length of the test section of 4.2 m. Absorption signals were measured through quartz windows near to the end plate of the tube. In measurements of HO_2- and H_2O_2-concentration profiles, the light source was a continuous Xe high pressure arc lamp. Measurements of HO profiles were done using a ring laser. More details of our shock tube and the applied technique are mentioned, e.g., in Refs. 8, 14, and 15, and are not repeated here.

In the first high temperature study[8] of reaction (1), HO_2 was produced via the reaction sequence

$$H_2O_2 + M \rightarrow 2HO + M, \quad (4)$$

$$HO + H_2O_2 \rightarrow H_2O + HO_2. \quad (3)$$

In the present work, HO_2 was also formed via the reaction

$$H + O_2 + M \rightarrow HO_2 + M. \quad (7)$$

A clean source of H atoms under medium temperature conditions was found in the decomposition of dimethylperoxide

$$CH_3O_2CH_3 + M \rightarrow 2CH_3O + M \quad (8)$$

which is followed by the rapid decomposition of methoxy radicals

$$CH_3O + M \rightarrow CH_2O + H + M. \quad (9)$$

As long as CH_2O does not interfere with the HO_2 reactions, this method proved to provide a particularly clean access to reaction (1). [The reaction $CH_3O + O_2 \rightarrow HO_2 + CH_2O$ is also known to produce HO_2. It was included in the modeling, but under our conditions its rate constant is too small for a competition of this reaction with reaction (9), see Table II.]

Dimethylperoxide was produced by the method described in Ref. 16 using a flow of He and purification by repeated trap-to-trap distillation. Dimethylperoxide is known to decompose cleanly via reaction (8) to CH_3O at relatively low temperatures.[16–19] The subsequent decomposition of CH_3O via reaction (8) was also studied recently[20] such that this system presents a well characterized H atom source for relatively low temperature shock wave conditions. With an excess of O_2, HO_2 is then formed rapidly in large quantities such that reaction (1) can be studied easily by monitoring HO_2 absorption-time profiles. Figure 1

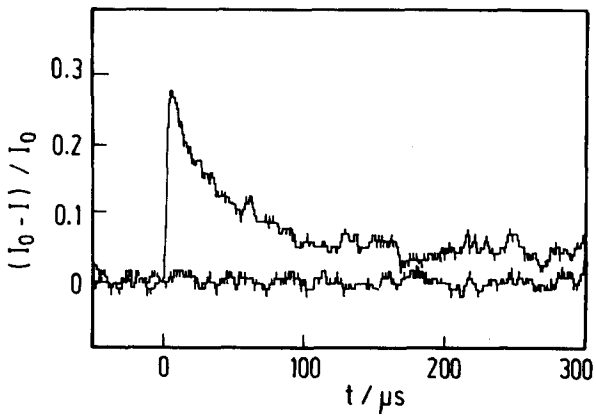

FIG. 1. Absorption-time profile of HO_2 disappearance via self-reaction (1) (reaction mixture of $[(CH_3O)_2]_{t=0} = 6.5\times10^{-8}$ mol cm^{-3}, $[O_2]_0 = 1.6\times10^{-6}$ mol cm^{-3}, and $[Ar] = 7.9\times10^{-5}$ mol cm^{-3}; $T = 970$ K; HO_2 absorption signal at 230 nm; I = transmitted light intensity, I_0 = incident light intensity).

shows an oscillogram recorded at 230 nm. This wavelength was chosen because of the optimum signal/noise ratios. Furthermore, at this wavelength the absorption coefficients ϵ of HO_2 and H_2O_2 are both nearly independent of the temperature between 300 and 1200 K; because of the larger value of $\epsilon(HO_2,\ 230\ nm) = 670\ l\,mol^{-1}\,cm^{-1}$ compared to $\epsilon(H_2O_2, 230\,nm) = 641\,mol^{-1}\,cm^{-1}$ (see Ref. 15), there is only very little perturbation of the HO_2 signal by H_2O_2 absorption. In order to confirm the identity of the species absorbing at 230 nm, we controlled the wavelength dependence of the maximum absorption level in oscillograms like Fig. 1. Figure 2 shows the result. The absorption coefficient (calibrated via that at 230 nm) follows that of HO_2 such as determined for 1000 K in Ref. 15. Figure 1 also confirms the second order character of the HO_2 decay; evaluation of the absorption-time profiles directly leads to the ratio $k_1/\epsilon(HO_2)$ from which we deduced k_1 using the absorption

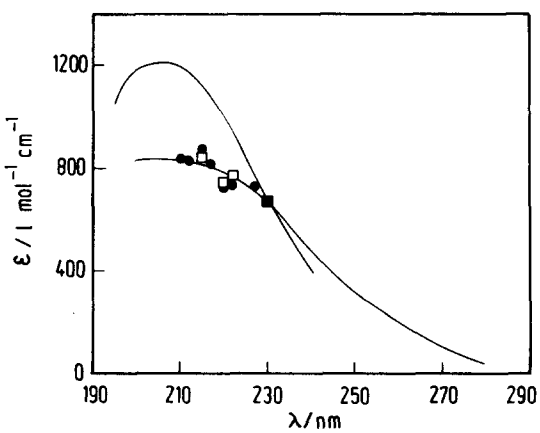

FIG. 2. HO_2 absorption coefficients in the UV (full lines: spectrum from Ref. 15 at 300 K ($\epsilon_{max} = 1200\,l\,mol^{-1}\,cm^{-1}$) and 1100 K ($\epsilon_{max} = 830\,l\,mol^{-1}\,cm^{-1}$); □: this work, $T = 1000$ K, ϵ derived from k_1/ϵ plots using k_1/ϵ at 230 nm and $\epsilon(230\,nm)$ for calibration; ●: this work, $T = 1000$ K, ϵ derived from the maximum HO_2 absorption using $\epsilon(230\,nm)$ for calibration).

This article is copyrighted as indicated in the article. Reuse of AIP content is subject to the terms at: http://scitation.aip.org/termsconditions. Downloaded to IP: 130.102.42.98 On: Sun, 23 Nov 2014 05:25:21

coefficient $\epsilon(HO_2, 230\ nm) = 670\ l\ mol^{-1}\ cm^{-1}$. On the basis of earlier temperature and shock wave determinations, this value is estimated to be certain within $\pm 10\%$ (old measurements in Ref. 15 confirmed by new studies, see, e.g., Ref. 9). Variations of the concentration conditions in the range $[CH_3O]_2/[Ar] = (0.25\text{–}2)\times 10^{-3}$, $[O_2]/[Ar] = (2.2\text{–}55)\times 10^{-2}$, $[Ar] \approx (1\text{–}5)\times 10^{-5}$ mol cm^{-3} had no influence on the derived values of k_1.

We also repeated the H_2O_2 decomposition experiments from Ref. 8. In this case, a flow of Ar passed a two-stage saturator filled with H_2O_2 and carried the H_2O_2/Ar mixture through an inlet in the end plate into the shock tube. The whole system contained only glass, teflon, and aluminum components. Nevertheless, substantial wall adsorption and decomposition takes place. The resulting H_2O content of the mixture has to be taken into account when the precision of the temperature has to be better than 10 K. This was the case in studies of the thermal decomposition of H_2O_2, see Ref. 15. The concentration of the H_2O_2 introduced into the shock tube was determined directly before the shock by measuring the absorption at 230 nm. The same wavelength was chosen to monitor the superimposed H_2O_2 and HO_2 signals. At a wavelength of 290 nm, the H_2O_2 signals could be recorded without superimposed HO_2. Examples of HO_2 and H_2O_2 absorption profiles were shown in Ref. 8 and are not reproduced here. HO-absorption profiles recorded with a shock tube of 20 cm diameter were observed with a frequency-doubled ring laser at the $Q_1(4)$ line of HO near 308 nm using two traversals of the laser beam through this tube. For the applied conditions, an absorption coefficient of HO of about $\epsilon = 5.7\times 10^4\ l\ mol^{-1}\ cm^{-1}$ was calibrated via the thermal decomposition of HNO_3. The large value of ϵ allowed for a sensitive determination of the HO profiles. Figure 3 shows an example recorded at 1070 K.

III. RESULTS

We performed experiments with the $(CH_3O)_2/O_2$-system temperatures between 770 and 1075 K. The HO_2 decays, like Fig. 1, could well be represented by clean, second order rate laws. The resulting values of k_1 are shown in Fig. 4. There is clearly a positive temperature coefficient of k_1 for the full range of studied temperatures. A detailed simulation of the reaction mechanism (see below) indicated that the observed concentration profiles were practically not influenced by secondary reactions such that the measured apparent rate constants indeed correspond to k_1. Reaction (1) produces H_2O_2 which also absorbs in the UV. Since the absorption coefficient of H_2O_2 near 230 nm is 10 times smaller than that of HO_2, and since two HO_2 radicals produce one H_2O_2, the residual H_2O_2 absorption could be neglected.

In the present work we have restricted the H_2O_2 experiments to conditions where only reactions (1), (3), and (4) are relevant. This is the case at temperatures below about 1100 K. At higher temperatures, other reactions such as

$$HO + HO_2 \rightarrow H_2O + O_2, \qquad (10)$$

HO_2 thermal decomposition, and reactions of H atoms, also come into play. In order to remain in a range of a unique interpretation of our observations, we avoided such complications. Modeling of the concentration profiles (see below) indicates that in the applied temperature range 970–1120 K the time dependence of the HO_2 profiles essentially only depends on k_1 and k_4. Since k_4 is known very accurately from the reevaluated[15] results of Ref. 8, k_1 was easily fitted from the recorded HO_2 profiles. The time of reaching the HO_2 maximum and the height of the maximum (using the known HO_2 absorption coefficient) were the characteristic observables of this fit. Figure 4 includes the results. The agreement with the $(CH_3O)_2/O_2$ results is very satisfactory confirming the marked rise of k_1 at $T \geqslant 770$ K. The much more limited original results for k_1 from Ref. 8 also agree with the new determination within the error limits.

The time dependence and the height of the HO-absorption signals (like Fig. 3) provides a direct access to the values of k_3, k_4, and k_{10}. Since k_4 is known, k_3 and k_{10} could be fitted. Values of $k_3 = 3\times 10^{12}$ cm^3 mol^{-1} s^{-1} and $k_{10} = 3\times 10^{13}$ cm^3 mol^{-1} s^{-1} were obtained near 1100 K. The value for k_3 agrees with the older determinations from Refs.

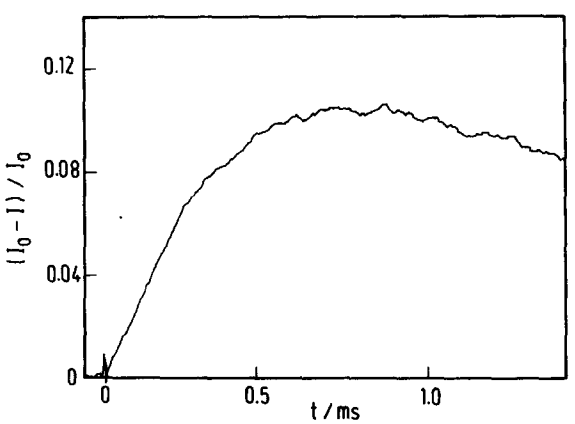

FIG. 3. Absorption-time profile of HO formation during the thermal decomposition of H_2O_2 ($T = 1070$ K, $[H_2O_2]_{t=0} = 1.25\times 10^{-9}$ mol cm^{-3}, $[Ar] = 2.4\times 10^{-6}$ mol cm^{-3}, absorption wavelength = 308.3278 nm, I = transmitted light intensity, I_0 = incident light intensity).

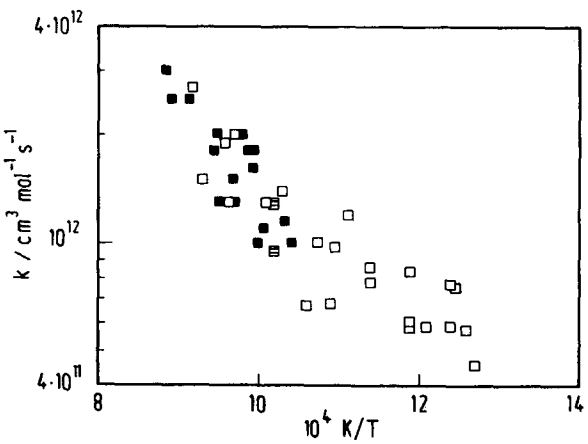

FIG. 4. Rate coefficients from the reaction $2HO_2 \rightarrow H_2O_2 + O_2$ (□: from experiments with $(CH_3O)_2/O_2$ mixtures; ■: from H_2O_2 thermal decomposition experiments).

This article is copyrighted as indicated in the article. Reuse of AIP content is subject to the terms at: http://scitation.aip.org/termsconditions. Downloaded to IP: 130.102.42.98 On: Sun, 23 Nov 2014 05:25:21

21–23, whereas the compilations of low temperature data from Refs. 1, 2, and 23 extrapolate to lower values near 1100 K. Our ring-laser experiments monitoring HO signals were not yet done with simultaneous measurements of H_2O_2 and HO_2 concentrations. Some uncertainties in the relevant H_2O_2 concentrations in the reaction mixture, therefore, remained in these experiments such that our determination of k_3 near 1100 K has an uncertainty of about a factor of 2. The value for k_{10} is consistent with the earlier estimate from Ref. 8 which was derived via the HO_2 profiles at $T > 1200$ K.

IV. SIMULATIONS OF COMPLETE MECHANISMS

In order to obtain undisputable values of k_1 and its temperature dependence, we intentionally restricted ourselves in this work to temperatures below 1100 K where only simple mechanism operate and unique determinations are possible. Nevertheless, perturbations from mechanistic complications had to be controlled. Table I shows the considered mechanism for the H_2O_2 system, Table II gives the additional reactions of the $(CH_3O)_2/O_2$ system.[24] Modeling of the $(CH_3O)_2/O_2$ system showed that the HO_2 profile after reaching the maximum indeed was not influenced by perturbing reactions. The mechanism only creates complicated concentration profiles in the first period of building up the HO_2 concentration, see Fig. 5. Shortly after reaching the HO_2 maximum, the HO_2 decay exclusively is governed by reaction (1). The $(CH_3O)_2/O_2$ system, therefore, proved to provide a clean HO_2 source which is not influenced by the presence of formaldehyde and methanol.

The numerical analysis of the concentration-time profiles of HO_2 in the H_2O_2 system confirmed that our observations here were free from complications up to about 1100 K. At higher temperatures the profiles rapidly become much more difficult to analyze. We are continuing to work into this range, in particular in order to specify k_{10} at $T > 1100$ K.

V. COMPARISON OF HIGH AND LOW TEMPERATURE VALUES OF k_1 WITH PREVIOUS MODELING RESULTS

A comparison of the present results with the recent medium and low temperature data from Refs. 9, 25, and 26 is given in Fig. 6. The present data overlap very well with the data from Ref. 9 and convincingly demonstrate the existence of a rate constant minimum near 700 K. Employing the recommended[1] low temperature expression of k_1, one may try to obtain a representation of the complete temperature dependence of k_1. At low temperatures and moderate pressures, the following expression was recommended in Ref. 1:

$$k_1 = 1.3\times10^{11}\exp(600\ \mathrm{K}/T)\ \mathrm{cm^3\ mol^{-1}\ s^{-1}} + [N_2]\,6.9\times10^{14}\exp(980\ \mathrm{K}/T)\ \mathrm{cm^6\ mol^{-2}\ s^{-1}}. \quad (11)$$

Polar third bodies, like H_2O instead of N_2, may strongly increase the second term. Under the present high temperature conditions, no pressure dependence of k_1 was noticed. For example, the 1 bar results from Ref. 9 agree with the present results for 5 bar. Using the 1 bar results from Eq. (11), between 300 and 1200 K and at 1 bar one obtains a general fit of k_1 of the form

$$k_1 = [4.2\times10^{14}\exp(-6030\ \mathrm{K}/T) + 1.3\times10^{11}\exp(+820\ \mathrm{K}/T)]\ \mathrm{cm^3\ mol^{-1}\ s^{-1}}. \quad (12)$$

Figure 6 compares this expression with the data from Refs. 9, 25, and 26.

A comparison of the available experimental results with theoretical model calculations so far appears unsatisfactory. The model from Ref. 6 qualitatively reproduces the observed behavior, see Fig. 7. It includes the pressure dependence at low temperatures which disappears at high temperatures; it also includes a rate constant minimum at high temperatures. However, the quantitative agreement with the experiments is not very good; in particular, the temperature coefficients of k_1 both in the low and high temperature ranges are too weak. The model of Ref. 7, on the other hand, provides a better description of the low temperature behavior whereas it fails to reproduce the high temperature turn up of k_1 (see Fig. 7). Apparently, the two models do not provide a sufficiently detailed account for the energy E and angular momentum J dependence of the specific rate constants for the formation of the $H_2O_4^*$ complex, its redissociation into two HO_2 radicals and its rearrangement and dissociation into $H_2O_2 + O_2$. Accounting for rotational effects in particular,[12,13] we are presently trying to arrive at a more successful modeling.

VI. CONCLUSIONS

By using two independent methods to generate HO_2 radicals under shock wave conditions, reaction (1) was shown to have a strong, positive temperature coefficient at $T > 770$ K. The combination with the recent data from Ref. 9 confirms a rate constant minimum near 700 K. Earlier low temperature studies[1,2] reported the observation of a pressure dependent and a pressure independent component of k_1. The importance of the former decreased with increasing

TABLE I. Rate coefficients relevant for the thermal decomposition of H_2O_2.

Reaction	Rate coefficient ($cm^3\ mol^{-1}\ s^{-1}$)	T(K)	Reference
$H_2O_2 + Ar \rightarrow 2HO + Ar$	$1.6\times10^{16}\exp(-21\,640\ \mathrm{K}/T)$	650–1100	15
$HO + H_2O_2 \rightarrow HO_2 + H_2O$	3.0×10^{12}	1100	This work
$HO_2 + HO_2 \rightarrow H_2O_2 + O_2$	$4.2\times10^{14}\exp(-6030\ \mathrm{K}/T) + 1.3\times10^{11}\exp(+820\ \mathrm{K}/T)$	300–1100 (1 bar Ar)	This work
$HO + HO_2 \rightarrow H_2O + O_2$	3.0×10^{13}	1100	This work

This article is copyrighted as indicated in the article. Reuse of AIP content is subject to the terms at: http://scitation.aip.org/termsconditions. Downloaded to IP: 130.102.42.98 On: Sun, 23 Nov 2014 05:25:21

TABLE II. Rate coefficients relevant for HO_2 reactions in $(CH_3O)_2/O_2$ mixtures (in addition to Table I, $k = A \exp(-B/T)$ $cm^3\ mol^{-1}\ s^{-1}$ from Ref. 24, except Ref. 20 for $CH_3O + M$.

Reaction	A	B(K)
$(CH_3O)_2 \rightarrow 2CH_3O$	5.2×10^{15}	18 690
$CH_3O + O \rightarrow CH_2O + OH$	6.0×10^{12}	0
$CH_3O + H \rightarrow CH_2O + H_2$	2.0×10^{13}	0
$CH_3O + M \rightarrow CH_2O + H + M$	9.5×10^{14}	10 340
$CH_3O + O_2 \rightarrow CH_2O + HO_2$	2.1×10^{11}	1720
$CH_3O + HCO \rightarrow CH_3OH + CO$	9.0×10^{13}	0
$CH_3O + CH_3O \rightarrow CH_2O + CH_3OH$	6.5×10^{13}	160
$CH_3O + CH_2O \rightarrow HCO + CH_3OH$	1.0×10^{11}	1500
$CH_3O + OH \rightarrow CH_2O + H_2O$	1.8×10^{13}	0
$CH_2O + OH \rightarrow HCO + H_2O$	2.6×10^{13}	400
$CH_2O + H \rightarrow HCO + H_2$	5.8×10^{13}	2280
$CH_2O + HO_2 \rightarrow HCO + H_2O_2$	7.0×10^{12}	6160
$CH_2O + HO_2 \rightarrow CH_2OH + O_2$	3.4×10^{12}	9620
$CH_2O + O \rightarrow HCO + OH$	4.1×10^{13}	1780
$CH_2OH + M \rightarrow CH_2O + H + M$	1.3×10^{15}	13 560
$CH_2OH + O_2 \rightarrow CH_2O + HO_2$	7.9×10^{12}	310
$CH_2OH + OH \rightarrow CH_2O + H_2O$	2.4×10^{13}	0
$CH_2OH + H \rightarrow CH_2O + H_2$	1.3×10^{13}	−10
$HCO + O_2 \rightarrow CO + HO_2$	4.8×10^{12}	120
$HCO + CH_3OH \rightarrow CH_2O + CH_2OH$	1.0×10^{14}	8690
$HCO + HCO \rightarrow CH_2O + CO$	1.6×10^{13}	−160
$HCO + OH \rightarrow CO + H_2O$	3.9×10^{13}	−120
$HCO + O \rightarrow CO_2 + H$	3.0×10^{13}	0
$HCO + O \rightarrow CO + OH$	3.0×10^{13}	0
$CH_3OH + O \rightarrow CH_2OH + OH$	1.3×10^{13}	2200
$CH_3OH + OH \rightarrow CH_3O + H_2O$	1.0×10^{13}	850
$CH_3OH + H \rightarrow CH_2OH + H_2$	3.7×10^{13}	2990
$CH_3OH + HO_2 \rightarrow CH_2OH + H_2O_2$	1.1×10^{12}	6980
$CH_3OH + OH \rightarrow CH_2OH + H_2O$	1.6×10^{13}	1050
$H + O_2 + M \rightarrow HO_2 + M$	1.5×10^{15}	−490
$H + O_2 \rightarrow OH + O$	1.3×10^{14}	7970

temperature such that pressure independent behavior of k_1 probably applies to shock wave conditions.

The present results appear of considerable importance for a better understanding of HO_2–H_2O_2 chemistry at temperatures around 1000 K. Reaction (1) here has served as the reference reaction;[5] increasing interest in high pressure combustion phenomena will lead even more attention towards reaction (1). With its well documented complicated temperature and pressure dependence, reaction (1) represents a prototype of a complex-forming bimolecular reaction. It shows one of the several possibilities of behavior which can be encountered with this type of reactions.[12] The "anomalous" properties have to be attributed to different features (energetic, rotational,[13] and vibrational[27,28]) at the entrance and exit activated complexes. In addition, the detailed effects of collisional transition probabilities in multichannel thermal[29] and chemical activation[30] systems have to be accounted for. Unfortunately, the corresponding reaction behavior cannot be predicted uniquely as long as the details of the potential energy surface are not known. Even the quantitative analysis on the basis of experimental results is not unique since several effects (rotational, energetic, and vibrational) in part compensate, in part produce similar behavior. This will be discussed in more detail in a forthcoming analysis[13] of complex-forming bimolecular reactions.

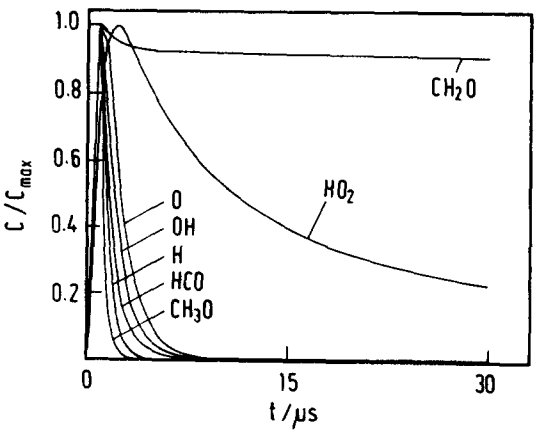

FIG. 5. Modeling of concentration-time profiles in $(CH_3O)_2/O_2/Ar$ mixtures ($T = 1000$ K, concentrations C in mol cm^{-3}: $[Ar] = 10^{-4}$, $[O_2]_{t=0} = 5\times10^{-6}$, $[(CH_3O)_2]_{t=0} = 10^{-7}$, $[CH_2O]_{max} = 1.23\times10^{-7}$, $[HO_2]_{max} = 5.1\times10^{-8}$, $[O]_{max} = 2.6\times10^{-9}$, $[HO]_{max} = 1.9\times10^{-9}$, $[H]_{max} = 2.9\times10^{-8}$, $[HCO]_{max} = 10^{-9}$, $[CH_3O]_{max} = 6.7\times10^{-8}$).

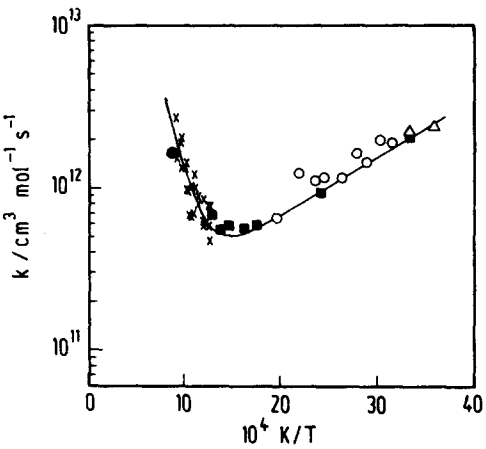

FIG. 6. Rate coefficients for the reaction $2HO_2 \rightarrow H_2O_2 + O_2$ [×: this work, ●: Ref. 8, ■: Ref. 9, O: Ref. 25, △: Ref. 26, —: fitted expression from Eq. (12)].

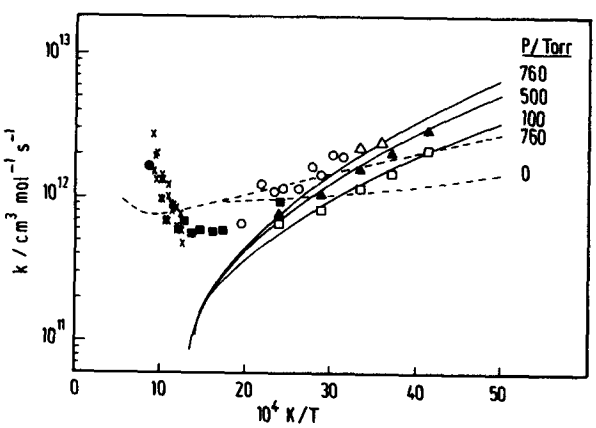

FIG. 7. Comparison of experimental and modeled rate coefficients for the reaction $2HO_2 \rightarrow H_2O_2 + O_2$ [experimental points as in Fig. 6 (1 atm), in addition ▲: Ref. 31, in 500 Torr of N_2, □: Ref. 31, in 100 Torr of N_2, —: modeling for 100, 500, and 700 Torr from Ref. 7, ---: modeling for 0 and 760 Torr from Ref. 6].

This article is copyrighted as indicated in the article. Reuse of AIP content is subject to the terms at: http://scitation.aip.org/termsconditions. Downloaded to IP: 130.102.42.98 On: Sun, 23 Nov 2014 05:25:21

ACKNOWLEDGMENTS

Financial support of this work by the Deutsche Forschungsgemeinschaft is gratefully acknowledged. The measurements of HO profiles have been made possible by the support from A. Hoffmann, H. Gg. Wagner, and R. Zellner. We are grateful for this as well as for the financial assistance from the Deutsche Forschungsgemeinschaft.

[1] R. Atkinson, D. L. Baulch, R. A. Cox, R. F. Hampson, J. A. Kerr, and J. Troe, J. Phys. Chem. Ref. Data **18**, 881 (1989), and earlier references cited therein.
[2] NASA Evaluation No. 8, W. B. DeMore, M. J. Molina, S. P. Sander, D. M. Golden, R. F. Hampson, M. J. Kurylo, C. J. Howard, and A. R. Ravishankara, JPL Pub. 87-41 (1987), and earlier references cited therein.
[3] W. J. Pitz, C. K. Westbrook, W. M. Proscia, and F. L. Dryer, 20th Symp. (Int.) on Combustion (Combustion Institute, Pittsburgh, 1985), p. 831; W. Pitz and C. K. Westbrook, Combustion and Flame **63**, 113 (1986).
[4] C. J. Jachimowski, Combustion and Flame **55**, 213 (1984).
[5] R. W. Walker, 22nd Symp. (Int.) on Combustion (Combustion Institute, Pittsburgh, 1988), p. 883.
[6] R. Patrick, J. R. Barker, and D. M. Golden, J. Phys. Chem. **88**, 128 (1984).
[7] M. Mozurkevich and S. W. Benson, Int. J. Chem. Kinet. **17**, 787 (1985).
[8] J. Troe, Ber. Bunsenges. Phys. Chem. **73**, 946 (1969).
[9] P. D. Lightfoot, B. Veyret, and R. Lesclaux, Chem. Phys. Lett. **150**, 120 (1988).
[10] S. E. Barlow, J. M. Van Doren, C. H. DePuy, V. M. Bierbaum, I. Dozan, E. E. Ferguson, N. G. Adams, D. Smith, B. R. Rowe, J. B. Marquette, G. Dupeyrat, and M. Durup-Ferguson, J. Chem. Phys. **85**, 3851 (1986).
[11] G. P. Smith, P. W. Fairchild, and D. R. Crosley, J. Chem. Phys. **81**, 2667 (1984).
[12] J. Troe, 22nd Symp. (Int.) on Combustion (Combustion Institute, Pittsburgh, 1988), p. 843.
[13] J. Troe, Int. J. Mass. Spectrosc. Ion Proc. **80**, 17 (1987). J. Chem. Phys., to be published
[14] D. C. Astholz, J. Troe, and W. Wieters, J. Chem. Phys. **70**, 5107 (1979).
[15] H. Kijewski and J. Troe, Helv. Chim. Acta **55**, 205 (1972).
[16] P. L. Hanst and J. G. Calvert, J. Phys. Chem. **63**, 104 (1959).
[17] J. R. Barker, S. W. Benson, and D. M. Golden, Int. J. Chem. Kinet. **9**, 31 (1977).
[18] L. Batt and R. D. McCulloch, Int. J. Chem. Kinet. **8**, 911 (1976).
[19] Y. Takezaki and C. Takeuchi, J. Chem. Phys. **22**, 1527 (1954).
[20] M. Page, M. C. Lin, Y. He, and T. K. Choudhhury, J. Phys. Chem. **93**, 4404 (1989).
[21] N. R. Greiner, J. Chem. Phys. **46**, 2795 (1967); J. Phys. Chem. **72**, 406 (1968).
[22] W. Hack, K. H. Hoyermann, and H. Gg. Wagner, Z. Naturforsch. Teil A **29**, 1236 (1974).
[23] I. A. Vardanyan, G. A. Sachyan, A. G. Philiposyan, and A. B. Nalbandyan, Combustion and Flame **22**, 153 (1974).
[24] W. Tsang and R. F. Hampson, J. Phys. Chem. Ref. Data **15**, 1087 (1986); NIST Chemical Kinetics Database Vers. 1.1, Release March 1989, The Office of Standard Reference Data, NIST Gaithersburg, MD 20899, USA.
[25] R. Patrick and M. J. Pilling, Chem. Phys. Lett. **91**, 343 (1982).
[26] B. Y. Andersson, R. A. Cox, and M. E. Jenkins, Int. J. Chem. Kinet. **20**, 283 (1988)
[27] J. Troe, J. Phys. Chem. **88**, 4375 (1984).
[28] C. J. Cobos, H. Hippler, and J. Troe, J. Phys. Chem. **89**, 342 (1985).
[29] Th. Just and J. Troe, J. Phys. Chem. **84**, 3068 (1980).
[30] J. Troe, J. Phys. Chem. **87**, 1800 (1983).
[31] C. C. Kircher and S. P. Sander, J. Phys. Chem. **88**, 2082 (1984).

This article is copyrighted as indicated in the article. Reuse of AIP content is subject to the terms at: http://scitation.aip.org/termsconditions. Downloaded to IP: 130.102.42.98 On: Sun, 23 Nov 2014 05:25:21